

Motor Eccentricity Fault Detection: Physics-Based and Data-Driven Approaches

Wang, Bingnan; Inoue, Hiroshi; Kanemaru, Makoto

TR2023-107 September 01, 2023

Abstract

Fault detection using motor current signature analysis (MCSA) is attractive for industrial applications due to its simplicity with no additional sensor installation required. However current components associated with faults are often very subtle and much smaller than the supply frequency component, making it challenging to detect and quantify fault levels. In this paper, we present our work on quantitative eccentricity fault diagnosis technologies for electric motors, including physical- model approach using improved winding function theory, which can simulate motor dynamics under faulty conditions and agrees well with experiment data, and data-driven approach using topological data analysis (TDA), which can effectively differentiate signals measured at different eccentricity levels. The advantages and limitations of each approach is discussed. Both methods can be extended to the detection and quantification of other types of electric motor faults.

IEEE International Symposium on Diagnostics for Electric Machines, Power Electronics and Drives (SDEMPED) 2023

Motor Eccentricity Fault Detection: Physics-Based and Data-Driven Approaches

Bingnan Wang

Mitsubishi Electric Research Laboratories
Cambridge, MA 02139 USA
bwang@merl.com

Hiroshi Inoue

Advanced Technology R&D Center
Mitsubishi Electric Corporation
Amagasaki, Hyogo 661-8661 Japan

Makoto Kanemaru

Advanced Technology R&D Center
Mitsubishi Electric Corporation
Amagasaki, Hyogo 661-8661 Japan

Abstract—Fault detection using motor current signature analysis (MCSA) is attractive for industrial applications due to its simplicity with no additional sensor installation required. However current components associated with faults are often very subtle and much smaller than the supply frequency component, making it challenging to detect and quantify fault levels. In this paper, we present our work on quantitative eccentricity fault diagnosis technologies for electric motors, including physical-model approach using improved winding function theory, which can simulate motor dynamics under faulty conditions and agrees well with experiment data, and data-driven approach using topological data analysis (TDA), which can effectively differentiate signals measured at different eccentricity levels. The advantages and limitations of each approach is discussed. Both methods can be extended to the detection and quantification of other types of electric motor faults.

Index Terms—Topic— *Electric motor, fault detection, eccentricity, winding function theory, topological data analysis*

I. INTRODUCTION

Eccentricity is one important indicator of mechanical faults in electric machines [1], [2]. Eccentricity happens as long as the stator and rotor are not concentric. Depending on the rotation profile of the rotor relative to the stator, the effect can be categorized into static eccentricity, dynamic eccentricity, and mixed eccentricity. In most practical cases, we encounter mixed eccentricity effect, which is a combination of both static and dynamic eccentricity [3], [4]. Eccentricity level of motors can increase over time due to a number of causes, such as the degradation of mechanical mounting structures and bearings. It is desirable to detect and fix defects in motors related to elevated eccentricity, as it can induce unbalanced magnetic pull, cause rubbing between stator and rotor surfaces, and eventually lead to motor failures and asset damages [5], [6].

Traditionally motor fault detection relies on sensing modalities such as vibration and acoustic emission [7], [8]. Mechanical faults including eccentricity can be related to the increased level of vibration amplitude, which can be measured by accelerometers mounted on the machines. However, such signals are often affected by various factors, such as the mounting location of the sensors, the vibration sources from other machines nearby on the factory floor, etc. It is therefore challenging to tell accurately whether there is a fault, let alone to quantify how severe the fault is.

Motor current signature analysis (MCSA) approach, on the other hand, has a few promising advantages compared with

other sensing methods, such as simple implementation and low cost [9], [10]. MCSA detects motor faults based on the measured motor current data, and requires no additional sensor installation. In the case of motor eccentricity fault, additional harmonic components will be induced in the permeance function and magnetic flux of the air gap, and show up in the induced voltage in the stator windings, and eventually in the stator current spectrum. With the understanding of the physical mechanism of faults, MCSA conducts detailed signal analysis, and relates the specific frequency components in the stator current spectrum to each type of fault. One main challenge with MCSA is that the fault signals are often much smaller and dominated by the fundamental component and its harmonics.

Fault detection techniques can be generally categorized into physics-based and data-driven approaches. For physics-based approach [7], [11]–[13], a physics-based model is established to describe the motor fault, which identifies detailed fault signatures, and the requirements on experiment measurements and data analysis in order to obtain and extract the required signals. On the other hand, data-driven approaches [8], [14], [15] rely on the available experiment data to train a data-driven model to make decisions on the motor fault condition. Both approaches have their own specific challenges in identifying eccentricity faults of electric motors.

A number of physics-based modeling approaches have been proposed for motor eccentricity fault analysis. The time-stepping finite-element method (TD-FEM) based simulation is accurate in calculating motor dynamic performance under eccentricity fault [12], [16]. The drawback of TD-FEM is its computational-intensive nature and long simulation time needed. Winding function based modeling techniques have also been developed to study motor faults [7], [13], [17]. The existing modified winding function method (MWFM) based models run faster than FEM, can identify frequency components related to faults, but cannot accurately calculate the amplitude of each component, due to the simplifications in the model.

For data-driven approaches, a lot of machine learning and deep learning algorithms have been applied to vibration signal based motor fault detection [8]. However, the fault signatures in the motor current are much smaller and more challenging to extract. Many algorithms effective for vibration signal based fault detection cannot extract features in the current signal

related to faults and distinguish current signals under different fault conditions. Domain knowledge of the fault physics, and involved signal analysis on the stator current spectrum are typically required to pre-process the obtained experiment data in order to identify and extract the fault features, before a data-driven model can be successfully established for fault detection and classification.

In this paper, we present both physics-based and data-driven approaches for effective eccentricity fault detection and quantification. For physics-based approach, we improve the modeling of eccentric motor with MWFM and take into consideration of slotting effect and saturation of the motor. The accuracy of the model is validated with experiment measurements. For data-driven approach, we apply topological data analysis (TDA) method for the effective extraction of features related to eccentricity fault in stator current signal without physical knowledge. The requirements, advantages, and limitations of each approach will be discussed.

The rest of the paper is organized as follows. In Section II, we first introduce an experiment setup to measure data of an induction motor at different eccentricity conditions, and provide an analysis to the obtained data. In Section III, we introduce the quantitative physics model for eccentric motor, and compare the simulation results with experiment. In Section IV, we present TDA and its application for eccentricity data processing and data-driven fault detection. In Section V, we discuss and summarize the differences between the two approaches. In Section VI we conclude the paper.

II. EXPERIMENT DATA ACQUISITION

A 0.75 kW, 3-phase squirrel-cage induction motor is modified for the experimental study, which has 2 pole pairs, 28 bars in the rotor, 36 slots in the stator, each has 37 turns of winding. In addition, the nominal air gap length is $g_0 = 0.28$ mm, air gap radius is $r = 41.6$ mm, and the stack length is $l = 80$ mm. The line-to-line voltage and frequency are 200 V and 60 Hz, respectively. In order to quantitatively study the behavior at different eccentricity levels, a few modifications have been made to the motor. As shown in Fig. 1, mounting structures are custom-made and used to replace the original bearings in the motor to support the rotor (only the mount on the load side is visible in the photo). The stator assembly of the motor is mounted on a linear stage, whose position in the horizontal direction, hence the eccentricity level, can be accurately adjusted using two pairs of micrometers mounted on each side of the linear stage. The load is provided by a powder brake.

With the modified motor setup, different static eccentricity levels in the horizontal direction can be created. In our experiment, a total of 6 eccentricity levels were created when the motor is stand still; data from phase current sensors and air gap sensors were recorded for each eccentricity level at 10 kHz sampling frequency under no-load condition. The eccentricity levels were set at 1.5%, 17.2%, 24.1%, 40.5%, 47.1%, 64.6% respectively, with percentage defined as the ratio of the maximum air gap deviation and the nominal air gap size. Our

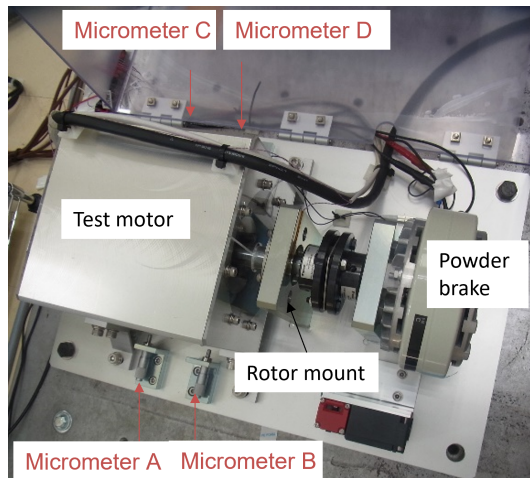


Fig. 1: The experiment setup for induction motor eccentricity study.

intention is to conduct experiments with multiple eccentricity levels from small to large. In addition to the pre-set static eccentricity, there is also a periodic oscillation for each gap sensor reading, indicating a small dynamic eccentricity level, which is around 6%. This mixed eccentricity effect creates side band signals in the current spectrum at $f_c = f_s \pm f_r$ and higher harmonics, where f_s is the supply frequency and f_r is the rotation frequency.

There is no significant change observed from the measured time-domain stator current data at different eccentricity levels. In order to understand and distinguish the data according to eccentricity level, typically detailed spectrum analysis is required. Fig. 2 shows the obtained spectrum using fast Fourier transform from measured phase A data of length 60 s. From the figure we can see that the frequency spectrum of the current are very similar for all cases, only the amplitudes of some components change with the different eccentricity level. To further understand the fault signatures and effectively determine the eccentricity condition based on these signatures, we can use physics-based models to identify and extract the fault components, or apply data-driven algorithms to extract fault features and distinguish these data.

III. PHYSICS-BASED ECCENTRICITY MODEL

In this work, we develop MWFM based simulation model for eccentric motor analysis, and the overall flow is described in Fig. 3. The simulation model takes in parameters including motor design parameters, supply voltage, load condition and fault condition, calculates the inductance terms between rotor and stator windings of the motor for each rotor position, and updates the dynamic signals during the operation of the motor including stator current, speed, and torque. Signal processing techniques such as FFT can be applied to the simulated stator current signal in order to obtain the spectrum. All signal components related to eccentricity faults can then be identified.

In this model, the motor dynamics are described by coupled circuit equations. For a 3-phase squirrel-cage induction motor,

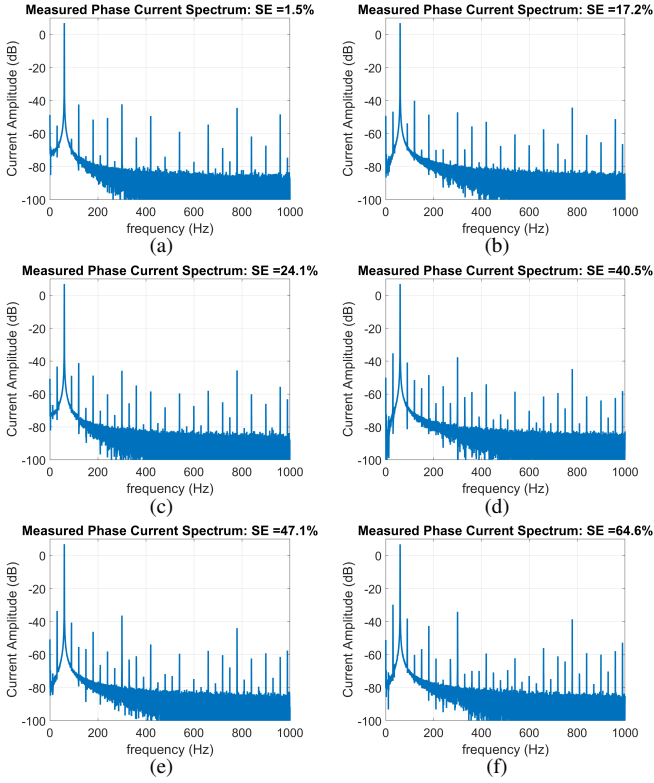


Fig. 2: Phase A current spectrum obtained from Fourier transform from the measured data at all six different eccentricity levels.

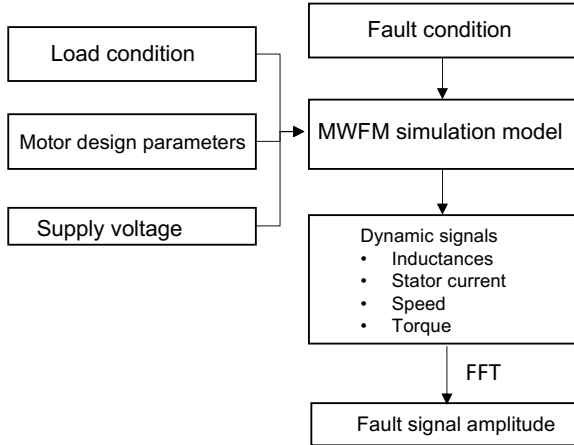


Fig. 3: The process of using MWFM based simulation model for the simulation and analysis of eccentric motor.

the stator voltage and flux linkage, rotor voltage and flux

linkage are described by the following equations respectively:

$$V_s = R_s I_s + \frac{d}{dt} \Lambda_s, \quad (1)$$

$$\Lambda_s = L_{ss} I_s + L_{sr} I_r, \quad (2)$$

$$V_r = R_r I_r + \frac{d}{dt} \Lambda_r, \quad (3)$$

$$\Lambda_r = L_{rs} I_s + L_{rr} I_r, \quad (4)$$

where V_s , V_r , I_s , I_r , R_s , R_r , Λ_s , Λ_r are the stator and rotor voltage, current, resistance, and flux linkage, respectively.

The electromagnetic torque is calculated by

$$T_e = \frac{1}{2} I_s^\top \frac{\partial L_{ss}}{\partial \theta_r} I_s + I_s^\top \frac{\partial L_{sr}}{\partial \theta_r} I_r + \frac{1}{2} I_r^\top \frac{\partial L_{rr}}{\partial \theta_r} I_r, \quad (5)$$

where θ_r is the rotor's mechanical angle. The mechanical equations are given as

$$\frac{d}{dt} \omega_r = \frac{1}{J} (T_e - T_L), \quad (6)$$

$$\frac{d}{dt} \theta_r = \omega_r, \quad (7)$$

where ω_r is the mechanical speed, T_L is the load torque, and J is the inertia.

Inductance terms and their derivatives are critical in determining the motor current and torque, as can be seen from equations (1) through (5). The calculation of inductances at each rotor position is done with MWFM, which calculates the inductance between two windings by the integration of the product of the two winding functions and the air gap permeance function, over all stator angles. For winding i and winding j , the inductance is evaluated as

$$L_{ij}(t) = \mu_0 l r \int_0^{2\pi} n_i(\phi, t) M_j(\phi, t) g^{-1}(\phi, t) d\phi, \quad (8)$$

where μ_0 is the free-space permeability, r is motor radius at the air gap, l is the stack length, $n_i(\phi, t)$ is the winding turns function for winding i , and $M_j(\phi, t)$ is the modified winding function for winding j . From the equation, we can see that the air gap function $g(\phi, t)$, which describes the spatial and temporal air gap profile, is especially important in calculating the motor performance under eccentricity conditions.

For a slotless motor, the air gap is uniform with nominal size denoted as g_0 . In actual induction motors, the slots in both stator and rotor effectively make the air gap length larger than g_0 . A Carter's coefficient K_c is introduced to represent the increase. The exact value of Carter's coefficient can be calculated based on the shape and geometrical parameters of the slots. Static eccentricity can be described by a time-invariant sinusoidal modulation to the air gap with amplitude denoted as δ_{SE} . Dynamic eccentricity introduces a time-varying modulation to the air gap function, and can be described by a sinusoidal function with amplitude denoted as δ_{DE} .

Under these conditions, the air gap function can be written as:

$$g(\phi, t) = g_0 K_c - \delta_{SE} g_0 \cos(\phi) - \delta_{DE} g_0 \cos(\phi - \omega_r t). \quad (9)$$

In addition, due to the nonlinear property of the iron core, saturation occurs at high flux density region, making the permeability lower than unsaturated case and non-uniformly distributed, and the effective inductance between windings smaller. We describe this saturation effect with a saturation factor k_{sat} [18], and apply it to the calculated inductance terms as obtained with equation (8). The exact value of the saturation factor depends on the geometrical design of the motor and the magnetic material properties, and can be pre-determined with numerical simulations. The process of identifying the model parameters is described in Ref. [19].

Dynamic simulations can then be conducted to obtain the motor current signals at each condition. Fig. 4 shows the simulated time-domain signal and the frequency spectrum of stator current at static eccentricity level of 40% and dynamic eccentricity level of 6%, together with the corresponding experiment data. We can see that the simulation results agree very well with the experiment data, especially the low-frequency side bands that are associated with eccentricity fault.

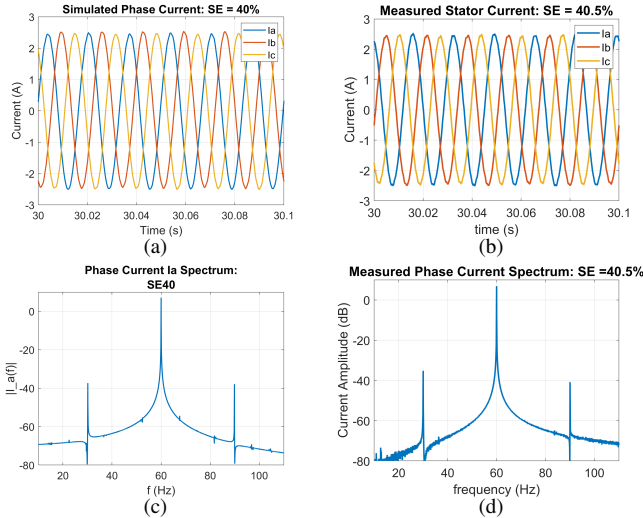


Fig. 4: The simulated (left) and corresponding experiment measurement (right) of phase current signal in time-domain (top), and the low-frequency components (bottom) of the spectrum obtained from Fourier transform at SE level of 40%.

We further run simulations with the model under different eccentricity conditions, obtain the stator current signals, and extract the frequency component at the side band of $f_s - f_r$. We use it as a fault indicator, and compare the simulated result with those obtained with experiment data. As shown in Fig. 5, very good match between MWFM simulation result and experiment data is achieved at different eccentricity levels.

We want to point out that the proposed physical model based on MWFM is not the only model for analyzing motor faults. Depending on the required accuracy and simulation time, available computation resources, we can choose the most suitable method. For example, if the accuracy is utmost important, then time-stepping finite-element simulations

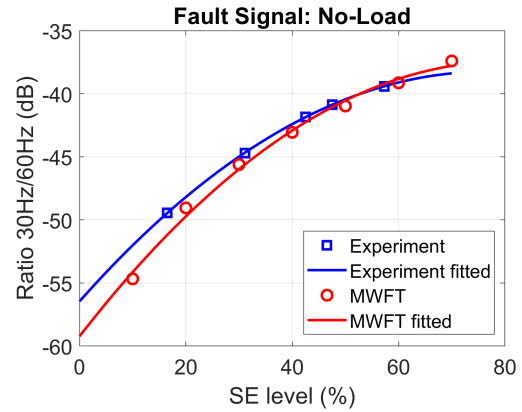


Fig. 5: MWFM simulation and experiment data comparison of the frequency component $f_s - f_r$ amplitude as function of eccentricity level.

should be used for the most detailed transient analysis of motors under faulty conditions. Simple harmonic analysis of faulty motor can be conducted analytically to identify the fault components. However, such analysis will not be able to provide quantitative accuracy of the amplitude of these fault components corresponding to the fault severity. In this regard, the MWFM simulation model provides a trade-off between computation complexity and quantitative accuracy in mapping the fault level with fault component amplitude.

While the simulation model based on MWFM approach is not exactly new, we have investigated in details how different aspects of the motor model, especially slotting effect and saturation effect, can affect the amplitude of frequency components related to eccentricity faults. We have also built a customized experiment setup to obtain measurement data and performed detailed spectrum analysis to validate the accuracy of the model. While there have been more involved modeling methods for saturation effect [18], we took a different approach by applying a correction factor to the calculated inductance values, which is simpler to implement with the MWFM model. We have demonstrated the effectiveness of the method with quantitative comparison of fault components in the stator current spectrum between simulation and experiment at different eccentricity levels.

IV. DATA-DRIVEN APPROACH WITH TOPOLOGICAL DATA ANALYSIS

On the other hand, the physics-based models, while accurate, do require detailed design parameters of the motor to achieve the accuracy. Such parameters are not always available, and complete physical model may not be able to be established to effectively perform fault detection tasks. Under these circumstances, we would like to explore data-driven approaches to address the problem by utilizing the available experiment data.

Since the eccentricity fault is highly sensitive and embedded in the current signal, it is challenging to apply the machine

learning and deep learning algorithms developed for vibration analysis directly [8]. Topological data analysis (TDA) offers a mathematical tool to extract the shape information from a given data space [20]. Largely driven by the recent development of persistent homology technique, TDA has been actively investigated for various data analysis tasks in different disciplines, from image analysis [21] and time-series data analysis [22], to chemistry [23], and material science [24]. TDA extracts the intrinsic shape information in a data space, and is robust to deformations and noises. While most TDA applications focus on discovering major shapes in the data and ignore smaller features, we show that the eccentricity fault information can be discovered in the smaller features in the stator current data, and can be reliably used for fault detection and quantification [25].

Simply speaking, persistent homology describes the evolution of topological features in a data space. In this study we focus on the low-dimensional features H_0 , which counts the number of connected components with increasing filtering radius ϵ . While more rigorous definitions and detailed descriptions are available elsewhere [26], a very high-level description of the calculation procedure is presented here:

- 1) Data points are sampled to form a point cloud. In our case, the point cloud of the time-domain 3-phase current data is naturally formed by taking a data segment and placing it in 3D Euclidean space.
- 2) Rips complex is constructed from the point cloud for a given threshold radius ϵ , which includes all topological features with pair-wise Euclidean distance between points no larger than ϵ .
- 3) The homology, which counts the number of topological features, is determined from the Rips complex.
- 4) Persistent homology is obtained by tracking the evolution of homology at different filtration radius ϵ .

Persistent homology can be represented and visualized in different ways. Here we describe it in the form of Betti sequence, which counts the number of features for a given range of filtration radius ϵ , and can be vectorized with fixed length for different data and suitable for machine learning studies.

Using the TDA procedure, Fig. 6 shows the computed H_0 Betti sequences of the phase current data measured at six different eccentricity levels. In each case, point cloud is formed from a total of 1,024 data points segmented from the three-phase stator current measurement, whose main topology is a circle in 3D space. When the filtration radius is $\epsilon = 0$, all data points are disconnected, hence the number of H_0 features is the same as the total data points of 1,024. With gradually increasing filtration radius, neighboring data points start to merge together, and the number of H_0 features monotonically decreases. Eventually with a large enough ϵ , all points are connected, and there is only one H_0 feature left. When eccentricity level is smaller, the data points are closer to a perfect circle defined by the fundamental component. When the eccentricity level increases, the data points deviate further from the circle,

and the distance between neighboring data points increases. Hence H_0 features can stay longer before merged together. Therefore, the area under Betti curve increases with increasing eccentricity level. The thresholded Betti curve effectively filters out the large fundamental component without a physical model.

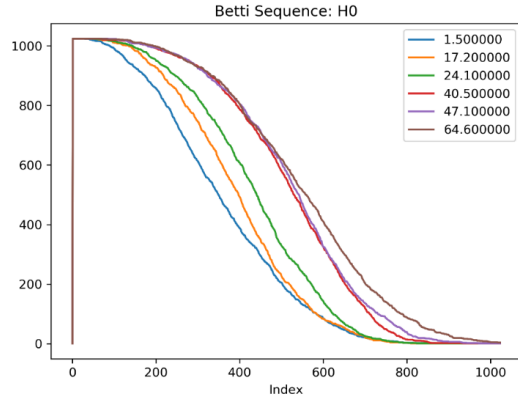


Fig. 6: The calculated H_0 Betti sequence from time-domain data samples of different eccentricity levels.

We can further quantitatively evaluate the similarity of the obtained Betti curves with pair-wise Euclidean distance, which is defined as

$$d_{\alpha\beta} = \sqrt{\sum_{i=1}^N (|\alpha_i - \beta_i|)^2}, \quad (10)$$

where α and β represent two Betti curves, and N is the total length of each curve. Smaller $d_{\alpha\beta}$ value indicates similar curves α and β and vice versa.

TABLE I: Pairwise Euclidean Distance between H_0 Betti sequences of different Eccentricity Levels

Eccentricity Level	1	2	3	4	5	6
1 (1.5%)	0	1832	3525	7000	7248	7836
2 (17.2%)	1832	0	1921	5648	5929	6609
3 (24.1%)	3525	1921	0	3813	4116	4913
4 (40.5%)	7000	5648	3813	0	452	1544
5 (47.1%)	7248	5929	4116	452	0	1196
6 (64.6%)	7836	6609	4913	1544	1196	0

Table I shows the calculated Euclidean distance between each pair of Betti curves generated from measurement data at six different eccentricity levels. It is clearly seen that the Euclidean distance between the H_0 curve associated with the smallest eccentricity level of 1.5% and other curves increases monotonically with increasing eccentricity level. Similar behaviour is seen from the table between Betti curves of different eccentricity levels: the larger the difference in eccentricity levels, the larger the Euclidean distance between their corresponding Betti curves.

From Fig. 6 and Table I, we can see that the proposed TDA approach can effectively distinguish very similar data sampled from different conditions, and correlate the topological feature with fault severity.

TABLE II: Eccentricity Level Prediction Performance with Trained Regression Model

Training Data	RMSE (%)	MAE (%)
Time-domain data	29.3	28.3
H_0 sequence	8.6	7.1

With the capability of effectively separating data from different eccentricity conditions, the extracted TDA features can be used to train machine learning models for fault prediction and quantification. A practical application scenario is to train a model based on existing measurement data, and make predictions when a new measurement is received at a later time, when the fault level is most likely higher. To mimic this task, we train a model using only measurement data from the four smaller eccentricity levels, and use the data from two larger eccentricity levels to test the prediction accuracy of the trained model.

For comparison, a quadratic regression model is trained with time-domain stator current data and the transformed H_0 Betti sequence data respectively. The prediction results are shown in Table II, where RMSE represents root-mean-square error and MAE represents mean absolute error. Model trained with time-domain data fails to make reasonable predictions as both errors are close to 30%. On the other hand, model trained with TDA data makes much more accurate predictions, with RMSE and MAE both below 10%, showing the effectiveness of the proposed method.

V. DISCUSSIONS

From the above investigation, we can see that by exploring motor physics with available motor design parameters, very good accuracy can be achieved for motor with eccentricity faults. Other than the good accuracy, one main advantage of the physics-based model is its generality and transferability. The model can be easily updated for the same motor under different load profile and fault conditions, and applied to a new motor with different parameters. The fault signals from the model are also easily explainable. Therefore, physics-based modeling should be the first choice when motor design parameters are available when dealing with fault detection problems.

Compared with physical-model based MCSA, which requires extensive domain knowledge in electric machines, and detailed design parameters to be able to identify and quantify fault signatures, no knowledge of the motor physics is required for the data-driven approach based on TDA. In addition, the prediction accuracy is achieved using a short data segment of around 0.1 s with trained model, while conventional frequency analysis techniques require at least a few seconds to tens of seconds data in order to resolve the fault components in frequency domain. These advantages make TDA based method especially suitable for fault detection purposes when design parameters for physical model are not available, while experiment data is available. Their comparisons are summarized in Table III.

Physics models can be established for other types of motor faults. As a mathematical tool, the TDA method could also be extended to the detection and classification of other types of motor faults. As future work, we will explore both methods for other fault types. We will establish physics models and evaluate the topological features of various motor faults, including H_0 and other features, compare them with the features obtained from eccentricity fault conditions, and examine the capability of TDA to discriminate different types of faults.

VI. CONCLUSIONS

In this paper, we presented and compared two types of approaches for motor eccentricity fault detection and quantification. For physics-based modeling approach, we improved the accuracy of modified winding function method by accounting for the motor physics including slotting and saturation effects. Dynamic simulations conducted with the model can obtain stator current data under various conditions, and achieve quantitative agreement with experiment data when comparing the extracted fault component related to eccentricity. For data-driven approach, we proposed topological data analysis method to effectively extract features related to eccentricity fault and distinguish data from different eccentricity levels, achieved without physical model. Physics models can easily adapt to new faults and new motors by updating design parameters and conditions, and should be the first choice when dealing with fault detection tasks. When motor design information is not readily available, data-driven approach is more suitable. We showed that TDA based data-driven models can be developed to effectively perform eccentricity fault detection and prediction. Both approaches can be extended to other fault classification and quantification tasks.

ACKNOWLEDGEMENT

The authors thank Lei Zhou, Mesaad W. Albader, AKM Khaled Ahsan Talukder, and Chungwei Lin for helpful discussions.

REFERENCES

- [1] M. E. H. Benbouzid, "A review of induction motors signature analysis as a medium for faults detection," *IEEE transactions on industrial electronics*, vol. 47, no. 5, pp. 984–993, 2000.
- [2] S. Nandi, H. A. Toliyat, and X. Li, "Condition monitoring and fault diagnosis of electrical motors—a review," *IEEE transactions on energy conversion*, vol. 20, no. 4, pp. 719–729, 2005.
- [3] S. Nandi, R. M. Bharadwaj, and H. A. Toliyat, "Performance analysis of a three-phase induction motor under mixed eccentricity condition," *IEEE Transactions on Energy Conversion*, vol. 17, no. 3, pp. 392–399, 2002.
- [4] H. A. Toliyat, S. Nandi, S. Choi, and H. Meshgin-Kelk, *Electric machines: modeling, condition monitoring, and fault diagnosis*. CRC press, 2012.
- [5] W. T. Thomson and I. Culbert, *Current signature analysis for condition monitoring of cage induction motors: Industrial application and case histories*. John Wiley & Sons, 2017.
- [6] X. Li, Q. Wu, and S. Nandi, "Performance analysis of a three-phase induction machine with inclined static eccentricity," *IEEE Transactions on Industry Applications*, vol. 43, no. 2, pp. 531–541, 2007.
- [7] S. Nandi, S. Ahmed, and H. A. Toliyat, "Detection of rotor slot and other eccentricity related harmonics in a three phase induction motor with different rotor cages," *IEEE Transactions on Energy Conversion*, vol. 16, no. 3, pp. 253–260, 2001.

TABLE III: Comparison of physical-model and TDA approaches for motor fault detection

Metric	Physical model	TDA
Require domain knowledge?	Yes	No
Require motor design parameters?	Yes	No
Require labelled data?	No	Yes
How to distinguish faults?	Spectral components	Topological features of point cloud
Explanability	Clear explanation with physics	Less clear explanation
Generalization capability	Can extend to other motors with new parameters	Need new data

- [8] S. Zhang, S. Zhang, B. Wang, and T. G. Habetler, "Deep learning algorithms for bearing fault diagnostics—a comprehensive review," *IEEE Access*, vol. 8, pp. 29 857–29 881, 2020.
- [9] J. Faiz and B. M. Ebrahimi, "Static eccentricity fault diagnosis in an accelerating no-load three-phase saturated squirrel-cage induction motor," *Progress in electromagnetics research*, vol. 10, pp. 35–54, 2008.
- [10] M. Akar, "Detection of a static eccentricity fault in a closed loop driven induction motor by using the angular domain order tracking analysis method," *Mechanical Systems and Signal Processing*, vol. 34, no. 1-2, pp. 173–182, 2013.
- [11] H. A. Toliyat, M. S. Arefeen, and A. G. Parlos, "A method for dynamic simulation of air-gap eccentricity in induction machines," *IEEE transactions on industry applications*, vol. 32, no. 4, pp. 910–918, 1996.
- [12] J. Faiz, B. M. Ebrahimi, B. Akin, and H. A. Toliyat, "Comprehensive eccentricity fault diagnosis in induction motors using finite element method," *IEEE Transactions on Magnetics*, vol. 45, no. 3, pp. 1764–1767, 2009.
- [13] L. Zhou, B. Wang, C. Lin, H. Inoue, and M. Miyoshi, "Static eccentricity fault detection for psh-type induction motors considering high-order air gap permeance harmonics," in *2021 IEEE International Electric Machines & Drives Conference (IEMDC)*. IEEE, 2021, pp. 1–7.
- [14] S. Zhang, F. Ye, B. Wang, and T. G. Habetler, "Semi-supervised bearing fault diagnosis and classification using variational autoencoder-based deep generative models," *IEEE Sensors Journal*, vol. 21, no. 5, pp. 6476–6486, 2021.
- [15] —, "Few-shot bearing fault diagnosis based on model-agnostic meta-learning," *IEEE Transactions on Industry Applications*, vol. 57, no. 5, pp. 4754–4764, 2021.
- [16] A. Sapena-Bano, M. Riera-Guasp, J. Martinez-Roman, M. Pineda-Sanchez, R. Puche-Panadero, and J. Perez-Cruz, "Fem-analytical hybrid model for real time simulation of ims under static eccentricity fault," in *2019 IEEE 12th International Symposium on Diagnostics for Electrical Machines, Power Electronics and Drives (SDEMPED)*. IEEE, 2019, pp. 108–114.
- [17] N. A. Al-Nuaim and H. Toliyat, "A novel method for modeling dynamic air-gap eccentricity in synchronous machines based on modified winding function theory," *IEEE Transactions on energy conversion*, vol. 13, no. 2, pp. 156–162, 1998.
- [18] J. C. Moreira and T. A. Lipo, "Modelling of saturated ac machines including air gap flux harmonic components," *Conference Record of the 1990 IEEE Industry Applications Society Annual Meeting*, pp. 37–44 vol.1, 1990.
- [19] B. Wang, M. W. Albader, H. Inoue, and M. Kanemaru, "Induction motor eccentricity fault analysis and quantification with modified winding function based model," in *2022 25th International Conference on Electrical Machines and Systems (ICEMS)*, 2022, pp. 1–6.
- [20] C. Gunnar, "Topology and data," *Bulletin of the American Mathematical Society*, vol. 46, no. 2, pp. 255–308, 2009.
- [21] T. Qaiser, Y.-W. Tsang, D. Taniyama, N. Sakamoto, K. Nakane, D. Epstein, and N. Rajpoot, "Fast and accurate tumor segmentation of histology images using persistent homology and deep convolutional features," *Medical image analysis*, vol. 55, pp. 1–14, 2019.
- [22] Y. Umeda, J. Kaneko, and H. Kikuchi, "Topological data analysis and its application to time-series data analysis," *Fujitsu Scientific & Technical Journal*, vol. 55, no. 2, pp. 65–71, 2019.
- [23] Y. Lee, S. D. Barthel, P. Dlotko, S. M. Moosavi, K. Hess, and B. Smit, "Quantifying similarity of pore-geometry in nanoporous materials," *Nature communications*, vol. 8, no. 1, pp. 1–8, 2017.
- [24] Y. Hiraoka, T. Nakamura, A. Hirata, E. G. Escobar, K. Matsue, and Y. Nishiura, "Hierarchical structures of amorphous solids characterized by persistent homology," *Proceedings of the National Academy of Sciences*, vol. 113, no. 26, pp. 7035–7040, 2016. [Online]. Available: <https://www.pnas.org/content/113/26/7035>
- [25] B. Wang, C. Lin, H. Inoue, and M. Kanemaru, "Topological data analysis for electric motor eccentricity fault detection," in *IECON 2022 – 48th Annual Conference of the IEEE Industrial Electronics Society*, 2022, pp. 1–6.
- [26] H. Edelsbrunner, D. Letscher, and A. Zomorodian, "Topological persistence and simplification," in *Proceedings 41st annual symposium on foundations of computer science*. IEEE, 2000, pp. 454–463.

BIOGRAPHIES

Bingnan Wang received his B.S. degree from Fudan University, Shanghai, China, in 2003, and Ph.D. degree from Iowa State University, Ames, IA, USA, in 2009, both in Physics. He has been with Mitsubishi Electric Research Laboratories (MERL), located in Cambridge, Massachusetts since then, and is now a Senior Principal Research Scientist. His research expertise includes electromagnetic analysis and photonics, and has worked on projects from wireless power transfer, sensing, to electric machines, and energy systems. His current research focuses on electric machine analysis, design optimization, fault diagnosis with both physics modeling and machine learning techniques.

Hiroshi Inoue received B.E. and M.E. degree from The University of Tokyo, Japan, in 2012 and 2014, respectively. He has been a researcher at Mitsubishi Electric Corporation since April 2014. His primary research focus is motor malfunction diagnosis technology. He is currently a member of the Mitsubishi Electric Advanced Technology R&D Center, Electromechanical Systems Department.

Makoto Kanemaru received B.E., M.E. and Ph.D. degree from Tokyo Institute of Technology, Japan, in 2006, 2008 and 2011, respectively. He has been a researcher at Mitsubishi Electric Corporation since April 2011. From 2019 to 2020, he was a visiting scholar at Walter H. Shorenstein Asia-Pacific Research Center, Stanford University, USA. His primary research focus is motor malfunction diagnosis technology. He is currently a group manager in Electromechanical Systems Department of the Mitsubishi Electric Advanced Technology R&D Center.